Complex Pattern Formation of Simple Biochemical Amplification Reactions in Micro-Structured Flow Reactors

Jörg Ackermann[a], Thomas Kirner[b], and Sabine H. L. Klapp[c]

[a] Technical University of Applied Sciences Berlin, FB V, Bioinformatics, Seestraße 64, D-13347 Berlin, Germany
[b] FluIT Biosystems, Schloss Birlinghoven, D-53754 Sankt Augustin, Germany
[c] Stranski-Laboratorium für Physikalische und Theoretische Chemie, TC7, Technische Universität Berlin, Straße des 17. Juni 124, D-10623 Berlin, Germany

Reprint requests to Dr. J. A.; E-mail: joerg.ackermann@tfh-berlin.de

Z. Naturforsch. **61a,** 60 – 68 (2006); received December 16, 2005

We have studied the dynamics of a simple amplification reaction in micro-structured flow reactors. The autocatalytic amplification reaction $A + R \longrightarrow 2A$ serves as a model to describe the fundamental properties of amplification systems in an open reaction chamber. A constant inflow of resources R feeds the reaction and an outflow keeps the total mass constant. A characterization of the system in a well stirred reaction chamber is presented by discussing the steady states of the system and their bifurcation properties. In the non-stirred case, where the species diffuse freely in a spatially extended chamber, numerical solutions of a reaction-diffusion equation describe the dynamic behavior of the system. It turns out that inhibition reactions and death terms, which are unavoidable in micro-structured reaction chambers, play an essential role in the behavior of the system. The rich dynamical behavior shows three fundamental properties of non-variational nonlinear open systems: temporal order, such as limit cycle oscillation, spatially periodic order, and complex spatial-temporal pattern formation. The results are of special interest for recent experiments with evolutionary molecular ecosystems in micro-structured flow reactors.

Key words: Biochemistry; Amplification; Diffusion; Nonlinear Systems; Evolutionary Molecular Ecosystems.

1. Introduction

The reaction $A + R \longrightarrow 2A$, where an autocatalytic species A consumes a resource R for its own reproduction, is the most simple and fundamental model for exponential amplification and replication in chemical, biological, ecological, and micro-biological systems [1 – 5]. From the viewpoint of dynamical systems, however, this reaction is rather unspectacular [6, 7]. It shows neither limit cycle oscillation nor any pattern formation. Such complex behavior is more closely connected to higher order reactions [8 – 12] or reaction systems with more than two species [13 –16].

Exponential growth is a common feature of isothermal biochemical replication systems. Examples of such protein-mediated systems are the 3SR reaction [17 – 19], the NASBA system [20, 21], or the SDA reaction [22]. Exponential growth has also been demonstrated for protein-free systems like the ligase ribozyme cycle of Paul and Joyce [23] or the deoxyribozyme cycle based on cleavage of Levy and Ellington [24]. Experiments with simple molecular ecosystems [25 – 32] motivate the following question: Given a replication which could be described by the most simple autocatalytic reaction, how would it behave in a micro-structured flow reactor and what effects will have a major impact on its dynamical behavior?

In this context, inhibition reactions and death terms are present to a certain extent in any real biochemical amplification system, especially if it runs in a micro-structured reactor. From the experimental point of view, these effects are important not only because they are unavoidable, but also because such reactions may be easily enhanced by adding appropriate chemicals or enzymes to the inlet solution. Moreover, the diffusion constant of these reactants can be controlled by immobilizing them on micro-beads or applying micro-emulsion vesicles given to the inlet. Within limits these effects can be influenced by the experimentalist, and hence they may present valuable *Steuerparameters* to control the dynamic behavior of the system.

0932–0784 / 06 / 0100–0060 $ 06.00 © 2006 Verlag der Zeitschrift für Naturforschung, Tübingen · http://znaturforsch.com

The dynamics of biochemical replication systems play a key role concerning the persistence of functional cooperation in evolutionary systems, and the results presented here are of interest in the theory of evolutionary systems. Evolutionary aspects of biochemical systems, however, are beyond the scope of this work.

The paper is organized as follows. Section 2 starts with an introduction to the model. A bifurcation analysis gives a systematic exploration of the parameter space and characterizes the system in a well stirred flow reactor. Section 3 deals with the pattern formation behavior in spatially extended reactors. This section demonstrates the ability of the system to show stationary (Turing) patterns as well as spatial-temporal patterns. Section 4 briefly discusses the relevance of the results for experimental systems.

2. Well Stirred Flow Reactor

Assume an autocatalytic reaction consuming a resource

$$\mathrm{A} + \mathrm{R} \xrightarrow{k_1} 2\mathrm{A}, \tag{1}$$

where A and R denote the autocatalytic species and the resource, respectively. This reaction is the basic model for resource limited autocatalytic reactions or (isothermal) biochemical amplification reactions. The autocatalyst can be inhibited by an inhibitor I:

$$\mathrm{A} + \mathrm{I} \xrightarrow{k_2} \mathrm{A:I}. \tag{2}$$

The reaction may be reversible in general. Such an inhibition reaction can play a major role for reactions in micro-structured devices. The same is true for a death reaction

$$\mathrm{A} \xrightarrow{k} \tag{3}$$

in biochemical amplification reactions.

Let the system run in a well stirred reaction chamber with external inflow of resource R and inhibitor I. The inflow is compensated by an outflow term to keep the total mass constant. The full system has the form:

$$\begin{array}{lll} \mathrm{A}+\mathrm{R} & \xrightarrow{k_1} 2\mathrm{A} & \text{(autocatalysis)},\\ \mathrm{A}+\mathrm{I} & \xrightarrow{k_2} \mathrm{A:I} & \text{(inhibition)},\\ \mathrm{A} & \xrightarrow{F+k} & \text{(outflow and death)},\\ \mathrm{R},\mathrm{I},\mathrm{A:I} & \xrightarrow{F} & \text{(outflow)},\\ & \xrightarrow{F\,r_0} \mathrm{R} & \text{(inflow)},\\ & \xrightarrow{F\,i_0} \mathrm{I} & \text{(inflow)}, \end{array} \tag{4}$$

where r_0 and i_0 denote the concentration of resource and inhibitor in the inflow channel. The corresponding system of ordinary differential equations (ODE) reads

$$\begin{array}{rcrcrcl} \partial a/\partial\tau = & & a\,r & - & \alpha a\,i & - & (f+\kappa)\,a,\\ \partial r/\partial\tau = & - & a\,r & & & + & f\,(1-r),\\ \partial i/\partial\tau = & & & - & \alpha a\,i & + & f\,(i_0-i), \end{array} \tag{5}$$

where all concentrations are measured as multiples of the constant resource concentration r_0 in the inlet. The timescale is defined by the dimensionless time $\tau \equiv t\,k_1 r_0$. Other dimensionless parameters are $\alpha = k_2/k_1$, $f = F/(k_1 r_0)$, and $\kappa = k/(k_1 r_0)$. For simplicity we are considering an irreversible inhibition reaction.

The non-trivial fixed point concentration for a is given by

$$a_\pm = -p/2 \pm \left(p^2/4 - q\right)^{1/2}, \tag{6}$$

with

$$p = f\,[1 + 1/\alpha - (1-i_0)/(f+\kappa)] \tag{7}$$

and

$$q = f^2(i_0\alpha + f + \kappa - 1)/[\alpha(f+\kappa)]. \tag{8}$$

Before proceeding, let us discuss solution 6 qualitatively. Two fixed points emerge at the saddle node bifurcation ($q - p^2/4 = 0$) along the hyperplane (for $\alpha > 1$)

$$f = f_{\mathrm{saddle}}(\kappa,\alpha,i_0) = \alpha(1-i_0^{1/2})^2/(\alpha-1) - \kappa. \tag{9}$$

Two solutions evolve for slow flow rates $f < f_{\mathrm{saddle}}$ or a slow inhibition reaction $\alpha < 1$. In general these fixed points may be unphysical negative solutions. For $q < 0$, i.e. a sufficiently low inhibition rate,

$$\alpha < \alpha_{\mathrm{singlet}}(f,\kappa,i_0) = (1-f-\kappa)/i_0, \tag{10}$$

only one positive solution (a_+) exists.

Two positive non-trivial solutions will emerge at the saddle node bifurcation if, and only if, the concentration at the saddle node bifurcation $a = -p/2$ is positive. This gives a necessary condition for two positive non-trivial solutions

$$f < f_+(\kappa,\alpha,i_0) = \alpha(1-i_0)/(1+\alpha) - \kappa. \tag{11}$$

The second positive fixed point (a_-) emerges at the saddle node bifurcation $f = f_{\mathrm{saddle}}$ in the case of sufficiently low flow rate $f < f_+$. Note, however, that a_-

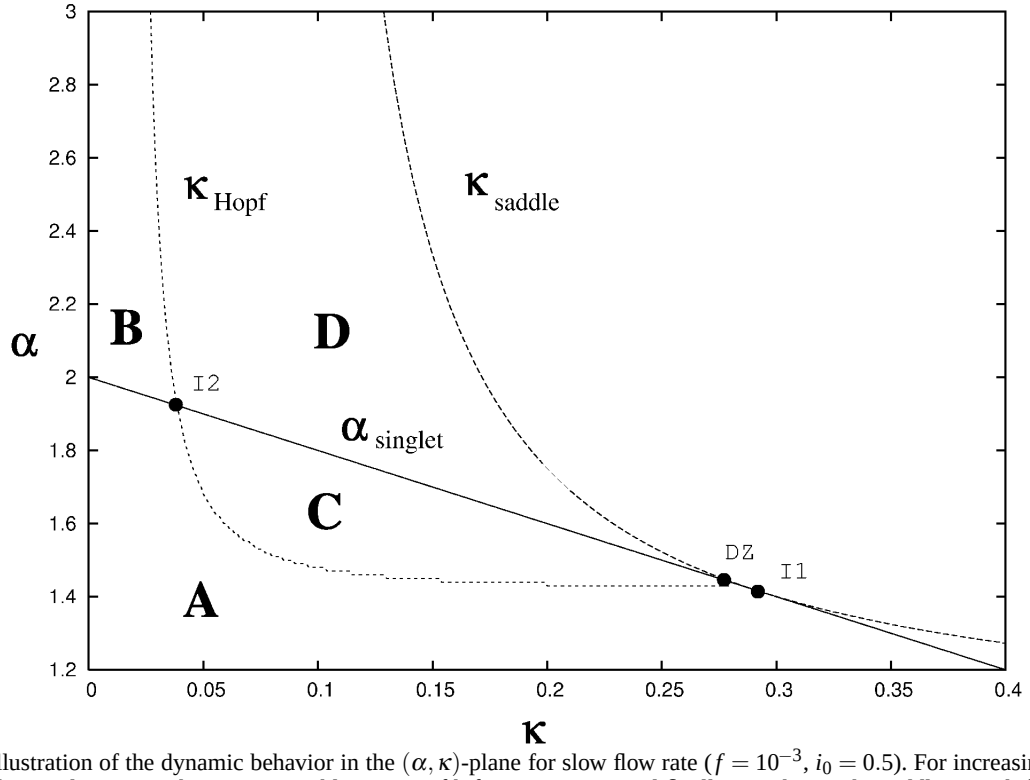

Fig. 1. Illustration of the dynamic behavior in the (α, κ)-plane for slow flow rate ($f = 10^{-3}$, $i_0 = 0.5$). For increasing death term κ the steady state a_+ becomes unstable at a Hopf bifurcation κ_{Hopf} and finally vanishes at the saddle point bifurcation κ_{saddle}. The Hopf bifurcation and the saddle point bifurcations meet at the double-zero codimension-2 point DZ. The point DZ is in close neighborhood of the point I1 where the transcritical bifurcation α_{singlet} intersect the saddle node bifurcation κ_{saddle}. A third point I2 describes the intersection of the transcritical bifurcation α_{singlet} and the Hopf bifurcation κ_{Hopf}. The domain $\kappa < \kappa_{\text{saddle}}$ is divided in four regimes (see Table 1): A, global attractor (a_+); B, bistable; C, oscillation; and D, global attractor (a_{tr}).

Death term	Inhibition rate	Fixed points with positive concentration	Dynamic behavior	Case
$0 \le \kappa < \kappa_{\text{Hopf}}$	$\alpha < \alpha_{\text{singlet}}$	a_+ stable a_{tr} unstable	global attractor (a_+)	A
	$\alpha_{\text{singlet}} < \alpha$	a_+ stable a_- unstable a_{tr} stable	bistable	B
$\kappa_{\text{Hopf}} < \kappa$	$\alpha < \alpha_{\text{singlet}}$	a_+ unstable a_{tr} unstable	oscillation	C
	$\alpha_{\text{singlet}} < \alpha$	a_+ unstable a_- unstable a_{tr} stable	global attractor (a_{tr})	D

Table 1. Variety of dynamic behavior of the system for various choices of the death term κ and the inhibition rate α, see Figure 1.

may become negative again for $\alpha < \alpha_{\text{singlet}}$. The condition for two non-trivial fixed points is a fast inhibition ($\alpha > \alpha_{\text{singlet}}$) combined with a low flow rate [$f < \min(f_{\text{saddle}}, f_+)$]. Note that α_{singlet}, f_{saddle}, and f_+ intersect at a joint coalescence point in the (κ, α)-plane (see I1 in Fig. 1):

$$(\kappa, \alpha) = (1 - \sqrt{i_0} - f, \quad 1/\sqrt{i_0}). \tag{12}$$

Let us now turn to the local stability of the fixed points. For the trivial fixed point ($a = 0$, $r = 1$, $i = i_0$) the Jacobian matrix of (5) has the intrinsic values

$$\lambda_{1,2} = -f, \quad \lambda_3 = (\alpha_{\text{singlet}} - \alpha) i_0. \tag{13}$$

A transcritical bifurcation appears at $\alpha = \alpha_{\text{singlet}}$. The trivial fixed point becomes unstable for low inhibition $\alpha < \alpha_{\text{singlet}}$, whereas simultaneously the non-trivial

fixed point a_- becomes negative (and stable, see below).

To obtain the linear stability of the non-trivial fixed points a numerical analysis of the Jacobian has to be performed. It turns out that the stability depends on the chosen set of parameters (α, f, i_0, κ) (see Table 1).

In the case of a zero death term ($\kappa = 0$) the situation is as follows: The positive branch of the non-trivial solution (a_+) is stable, whereas the trivial fixed point is either unstable for slow inhibition ($\alpha < \alpha_{\text{singlet}}$) or stable for fast inhibition ($\alpha > \alpha_{\text{singlet}}$). The second non-trivial fixed point (a_-) is unstable for $\alpha > \alpha_{\text{singlet}}$ and becomes negative and stable for $\alpha < \alpha_{\text{singlet}}$. Hence in the case of slow inhibition the state a_+ represents a global attractor, and the physical system will (for any initial condition $a > 0$) asymptotically end in this non-trivial fixed point. For fast inhibition, however, the system becomes bistable. The reaction can not commence for small initial concentrations of the autocatalyst, but may be ignited by a sufficient amount of initial concentration a. The unstable fixed point a_- represents a transition state between the stable trivial steady state a_{tr} and the stable non-trivial steady state a_+. Such behavior has also been observed for a cubic autocatalytic reaction of the type $2\text{A} + \text{R} \longrightarrow 3\text{A}$ [7, 33–36] or for the co-operative biochemical amplification reaction CATCH [16, 25].

The situation becomes more complicated for a non-zero death term ($\kappa > 0$). The non-trivial steady state a_+, which is always stable for $\kappa = 0$, may become unstable for $\kappa > 0$. The reaction is not able to compensate for the death term if either the inflow of new resources is very low (low f value) or if the flow rate is near its maximum critical value f_{critical}. The transition from a stable to an unstable steady state a_+ is described by a Hopf bifurcation κ_{Hopf}.

A different feature arises for weak inhibition. For $\alpha < \alpha_{\text{singlet}}$ the trivial fixed point a_{tr} becomes repulsive. Hence all fixed points become unstable for $\kappa > \kappa_{\text{Hopf}}$ and $\alpha < \alpha_{\text{singlet}}$. Consequently a limit cycle will emerge in this parameter region. Oscillatory behavior, however, is not restricted to weak inhibition. Limit cycles can also be observed for small inhibitor concentration i_0 and fast inhibition (data not shown).

Parameter regions corresponding to various dynamic scenarios are plotted in Fig. 1 for slow flow rate ($f = 10^{-3}$) and $i_0 = 0.5$. The Hopf bifurcation and the saddle point bifurcations meet at the point `DZ`. `DZ` at $\kappa_{\text{saddle}} \approx 0.2771$ and $\alpha_{\text{saddle}} \approx 1.446$ represents a double-zero codimension-2 point. A normal form analysis and the determination of an eventually existent homoclinic bifurcation is out of the scope of this work. This codimension-2 point `DZ` is in the close neighborhood of the point `I1` at $(\kappa, \alpha) = (1 - \sqrt{i_0} - f, 1/\sqrt{i_0}) \approx (0.2919, 1.446)$ where the transcritical bifurcation α_{singlet} intersect the saddle node bifurcation κ_{saddle}. At this coalescence point `I1` the Jacobian has the real eigenvalues $\lambda_1 = 0$, $\lambda_{1,2} = -f$. A third intersection point `I2` describes the crossing of the transcritical bifurcation α_{singlet} and the Hopf bifurcation κ_{Hopf}. Below the transcritical inhibition rate $\alpha < \alpha_{\text{singlet}} = (1.998 - 2\kappa)$ the trivial fixed point a_{tr} is unstable. Hence, the domain $\kappa < \kappa_{\text{saddle}}$ is divided in four regimes (see Table 1): A, global attractor (a_+); B, bistable; C, oscillation; and D, global attractor (a_{tr}).

3. Pattern Formation in Spatially Extended Reactors

To study the spatial behavior of the system, the ODE (5) have to be replaced by partial differential equations (PDE):

$$\begin{aligned} \partial a/\partial\tau &= \quad a\,r - \alpha a\,i - (f+\kappa)\,a + \nabla^2 a, \\ \partial r/\partial\tau &= -a\,r \qquad\quad + f\,(1-r) + d_r\nabla^2 r, \\ \partial i/\partial\tau &= \qquad -\alpha a\,i + f\,(i_0 - i) + d_i\nabla^2 i, \end{aligned} \tag{14}$$

where the dimensionless spatial coordinate is scaled by the length scale $l = [D_a/(k_1 r_0)]^{1/2}$ and the dimensionless diffusion constants are given by $d_r = D_r/D_a$ and $d_i = D_i/D_a$.

An important question is whether the system shows any Turing instability. A Turing instability is closely connected to time-independent patterns in spatially extended systems [37]. Note, however, that Turing patterns, i. e. patterns connected to a specific "chemical" wavelength, may also occur outside the region of classical Turing mechanisms [9].

A numerical investigation of the intrinsic values of the Jacobian shows that the homogenous steady state a_+ may become linear-unstable due to a Turing mechanism. Parameter regions where such Turing instabilities occur are plotted in Figure 2. For fast inhibition ($\alpha = 10$), Turing instabilities occur only in a narrow parameter region of the (α, κ)-plane near the coalescence point of the Hopf bifurcation and

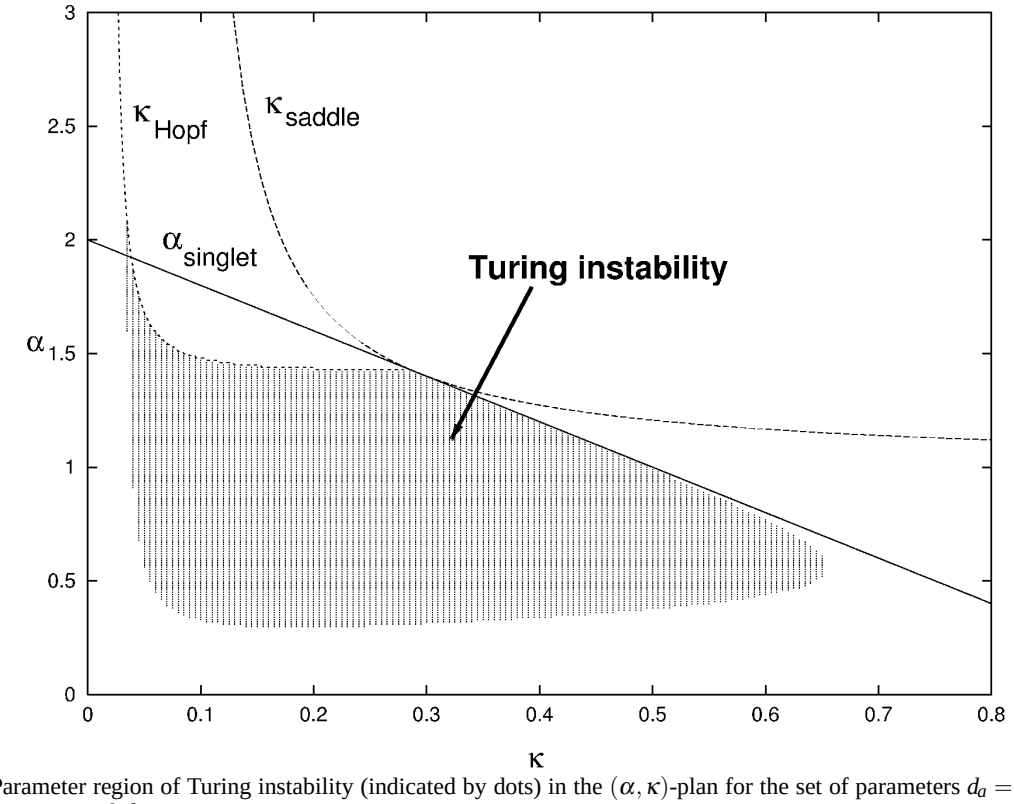

Fig. 2. Parameter region of Turing instability (indicated by dots) in the (α, κ)-plan for the set of parameters $d_a = 1$, $d_r = 2$, $d_i = 0$, $i_0 = 0.5$, and $f = 0.001$.

the saddle node bifurcation. The region of Turing instability becomes larger for increasing d_r and smaller for increasing d_i. For slow inhibition, the Turing instability can be observed in a rather broad region in the (α, κ)-plane, see Figure 2. No Turing mechanism was observed for the stable trivial steady state. The destabilization of homogeneous steady states arising from diffusion-driven spatial inhomogeneities can be demonstrated by numerical solutions of PDE (14). A forward Euler integration of the finite-difference equations, resulting from discretization of the diffusion operator, was performed. The spatial mesh consists of 256×256 grid points. The mesh size $\Delta x = 1$ and time steps of $\Delta t = 0.1$ are fine enough not to influence the result qualitatively. Periodic boundary conditions were applied.

An example of a Turing instability is shown in Figure 3 for fast inhibition $\alpha = 10$. The other parameters are $\kappa = 0.035$, $f = 0.06$, $i_0 = 0.5$, $d_i = 1$, and $d_r = 2$. The 2D grid was homogeneously initialized by the concentrations $a = 0.133884$, $r = 0.309464$, and $i = 0.021446$ disturbed by 1% random noise on each grid point. These concentrations present a homogeneous steady state, and the initial random noise in a spatially extended reactor would be damped away in the case of zero diffusion rates. A non-zero diffusion changes the dynamic behavior in the reactor. At around 300 time units the autocatalyst starts to grow at localized points to rather high concentration, accompanied by an extinction of the autocatalyst in other

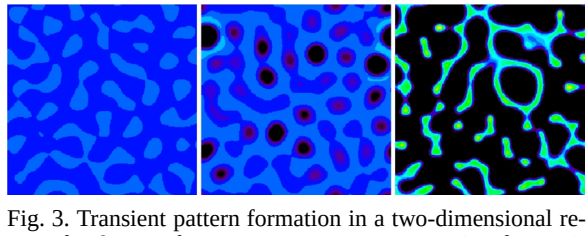

Fig. 3. Transient pattern formation in a two-dimensional reactor for the set of parameters: $\alpha = 10$, $\kappa = 0.035$, $f = 0.06$, $i_0 = 0.5$, $d_a = d_i = 1$, and $d_r = 2$. Images from left to right: $t = 300$, $t = 400$, and $t = 500$. The plot is rainbow color coded; black means $a = 0$ and red the highest concentration ($a = 0.43$). The Turing instability destabilizes the otherwise linear-stable steady state and the autocatalyst becomes extinct.

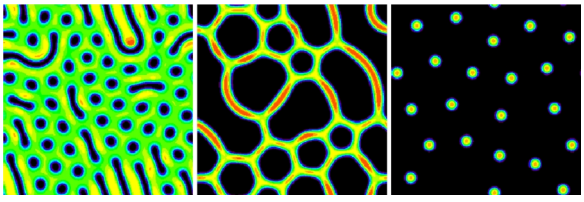

Fig. 4. Stationary patterns in a two-dimensional reactor for the set of parameters: $\alpha = 10$, $\kappa = 0.045$, $f = 0.049$, $i_0 = 0.5$, $d_a = 1$, $d_r = 2$ and various d_i. Images from left to right: $d_i = 0.0$, $d_i = 0.8$, and $d_i = 1.0$. The plot is rainbow color coded; black means $a = 0$ and red the corresponding highest concentration. The Turing instability destabilizes the homogenous steady state and stable spatial patterns emerge.

space regions, see Figure 3. In places of low autocatalyst concentration, the inhibitor concentration grows to its maximum value ($i = 0.5$). The local spots of high inhibitor concentration enlarge and the inhibitor displaces the autocatalyst to smaller and smaller space regions. Finally the autocatalyst disappeares, and the system approaches a homogeneous trivial steady state (not shown in Fig. 3).

The final collapse of the system into this trivial steady state can be prevented by a lower diffusion rate of the inhibitor. The dependence of the stationary pattern on the diffusion rate d_i is shown in Fig. 4 for a representative parameter set.

The patterns discussed above arise from steady states which are linearly stable in the well mixed case, but become unstable due to the ability of the system to form spatial patterns. These Turing patterns either collapse to the trivial (extinct) steady state, or they stabilize into a stationary spatial pattern. Numerical simulation was performed also outside the parameters region where the well stirred reactor shows (non-trivial) stable steady states. Homogeneous concentrations ($a = 0$, $i = i_0$) of the trivial steady state were chosen as initial condition. The reaction was initiated by a non-zero concentration of autocatalysts ($a = 0.2$, $i = 0.1$) located in a small rectangular space region (5×5 grid points) centered in the middle of the reactor. The initial concentrations on each grid point were disturbed by 1% random noise.

It turned out that the system shows a stationary pattern as well as a variety of spatial-temporal patterns in a rather broad parameter region. For fixed parameters $\alpha = 10$, $i_0 = 0.5$, $d_i = 0$, $d_r = 2$, for example, the system shows a pattern formation for death terms up to $\kappa = 0.25$. This is a surprising result, because this death term value is around five times larger than κ at the Hopf bifurcation or saddle node bifurcation. Turing-like stripe patterns and worm patterns were obtained for rather small death terms near the Hopf bifurcation, e. g. for values ($f = 0.06, \kappa = 0.04 - 0.06$), ($f = 0.04, \kappa = 0.05 - 0.08$), and ($f = 0.02, \kappa = 0.06 - 0.07$). Stationary dot patterns are dominant for large flow terms or large death terms, e. g. for values ($f = 0.06, \kappa = 0.07 - 0.14$), ($f = 0.04, \kappa = 0.15$), and ($f = 0.02, \kappa = 0.25$).

At intermediate death term values $\kappa \approx 0.09 - 0.2$ and low flow rate $f \leq 0.04$, oscillatory modi couple with the spatial pattern, producing in this way a variety of time-dependent spatial patterns. The typical period of the oscillatory Hopf modi decreases from around 200 time units at low flow rate ($f = 0.001$) to 80 time units for high flow rates ($f = 0.04$).

Dividing spot patterns were produced in the parameter region $f \leq 0.04$, $0.09 \leq \kappa \leq 0.11$. Such patterns were discussed by Pearson for the Gray-Scott model [9]. At larger values of the death term ($f \leq 0.04$, $0.12 \leq \kappa \leq 0.20$), oscillatory Turing patterns emerge. These patterns consist of moving and oscillating cells. Similar patterns have recently been reported as transition states to "twinkling eye" patterns in reaction-diffusion systems with two coupled layers, see [38].

4. Discussion

Our study shows that isothermal amplification reactions can produce a rich variety of complex behavior in a micro-structured flow reactor. Key roles for the dynamics of the system are played by inhibition reactions and death terms, which are unavoidable in micro-structured environments. This is particularly important for ongoing experiments involving simple molecular ecosystems [25 – 30, 32].

The simple model system studied in this work displays three fundamental properties of a non-variational nonlinear open system: temporal order, such as limit cycle oscillation, spatially periodic order, and complex spatial-temporal pattern formation. In a certain parameter regime oscillatory Turing patterns emerge. Oscillatory Turing instabilities have been found previously in a model for surface catalysis [39], in phase separating mixtures [40], in reactive Langmuir monolayers [41, 42], in Min-protein patterns in *Escherichia coli* [43 – 48] and in a model that mimics the Belousov-Zhabotinsky reaction in a system with two coupled layers [38].

We investigate the pattern formation behavior by extensive numerical simulation and give an example of a parameter region, where complex patterns emerge. We abstain from exploring the complex behavior of the system for the entire parameter space. Detailed studies are recommended for concrete experimental setups. Also, an analysis in terms of the nonlinear evolution equation for the amplitudes of the modes, the generalized Ginzburg-Landau equation, lies outside the scope of this work.

Biochemical amplification systems are very complex, but usually they can be approximated by a simple model describing exponential growth. This is the reasons why the "selection of the fittest" principle plays such an exceptional role in nature. This study shows that a simple three species system describing exponential growth shows Turing instability and complex spatiotemporal pattern formation in a broad parameter regime also outside the Turing instability regime. This result implies that any isothermal biochemical amplification reaction is able to produce such complex pattern formation in a micro-structured environment. Pattern formation has been regarded as a necessary characteristic for the emergence and persistence of cooperative function in evolutionary systems [3, 49 – 54] and hence is of relevance for the still open question of the origin of life as well as for the evolutionary optimization of complex function in molecular systems. In such systems the emergence of parasites plays an important role [31, 55].

How an experimental biochemical system has to be matched to such a simplifying model depends on the reaction conditions of the biochemical system, see for example [15]. Are the nucleotides (or some of the enzymes) fed in excess? Are surfaces of the reaction chamber preconditioned to minimize the immobilization of reactants to them? Is the diffusion of certain reactants (e. g. DNA, enzymes with various functions, nucleotides) restricted by micro-emulsion vesicles? Can reactants bind specifically to micro-particles diluted in the buffer solution?

Largely varying diffusion constants in or near an oscillatory medium usually give rise to Turing instabilities. Largely varying diffusion constants are common in biochemical systems as well, because enzymes are complex functional molecules and much bigger than nucleotides. Immobilizing reactants on beads or to the surface yield diffusion constants near zero. The choice $d_i = 0$, for example, corresponds to the case of an immobilized inhibitor in the reaction chamber. Although this is a natural choice for many experimental situations, this condition may not be valid in others.

Let us discuss the situation for the well-known isothermal 3SR amplification reaction. Typical doubling time periods in 3SR amplification reactions are in the range of 30 seconds up to a few minutes [56]. This determines the time unit in our simulations, and the expected period of the oscillatory mode would be in the order of 40 minutes to several hours. Typical diffusion rates of polynucleotides are in the order of $D_a = 2 \times 10^{-7}$ cm^2/s. Hence the length scale in our simulation grid is $l \approx 24$ μm, and a reactor size of 5×10^{-3} m would be sufficient to observe the predicted spatial structures with typical wave lengths in the range of 250 μm to 500 μm.

Experimentally one may choose either the enzymes or the nucleotides as "resource" just by feeding one of them in excess to the chamber. The diffusion rate of the resource R would be higher than the diffusion rate of the autocatalyst A, if the 3SR amplification rate is limited by the nucleotide concentration. This corresponds to an experimental setup where the enzymes are fed in excess into the flow chamber. The reverse is true if the reaction rate is limited by the concentration of one of the enzymes in the inlet flow. To obtain a diffusion rate of $d_i = 0$, the inhibitor has to be immobilized on micro-beads. Typical concentrations could be 10^{-6} M for the nucleotide and 5×10^{-7} M for the inhibitor to mimic the parameter regime discussed above. The effective amplification rate k_1 has to be in the order of magnitude of 3×10^4 M^{-1}s^{-1}. A realization of a fast inhibition reaction with $k_2 \approx 3 \times 10^5$ M^{-1}s^{-1} ($\alpha = 10$) should be possible by applying hybridization reactions to polynucleotide primers immobilized on beads. The RNaseH activity of the enzymes may be utilized to obtain small death terms in the range of $k = 1/3000$ s^{-1} to $k = 1/300$ s^{-1}. Assuming a micro-structured reactor, as described in [32], low pump rates in the range of 1 μl/25 min to 1 μl/2 h must be applied. Since the predicted concentration fluctuations are large (10^{-7}M-5×10^{-7} M) standard optical detection methods can be employed. In conclusion, the detection of complex behavior can be predicted for biochemical amplification reactions. Small structures and long-term experiments of several days to weeks must be envisaged for this technical task.

Acknowledgement

Part of this work was done at the former German National Research Center for Information Technology (GMD) now the Fraunhofer Gesellschaft. We thank J.S. McCaskill for helpful discussions and the referee for his thorough reading of the manuscript and his profound comments.

[1] J. M. Emlen, Population Biology, Macmillan Publishing Company, New York 1984.
[2] M. C. Cross and P. C. Hohenberg, Rev. Mod. Phys. **65**, 851 (1993).
[3] I. A. Hanski and M. E. Giplin, Metapopulation Biology, Academic Press, San Diego, CA 1997.
[4] R. M. May, Stability and Complexity in Model Ecosystems, Princeton University Press, Princeton, New Jersey 2001.
[5] J. D. Murray, Mathematical Biology, 3rd. ed., Springer, Berlin 2002.
[6] J. H. Merkin, D. J. Needham, and S. K. Scott, Proc. R. Soc. Lond. A **424**, 187 (1989).
[7] S. K. Scott and K. Showalter, J. Phys. Chem. **96**, 8703 (1992).
[8] A. Gierer and H. Meinhardt, Kybernetik **12**, 30 (1972).
[9] J. W. Pearson, Science **261**, 189 (1993).
[10] Th. Wilhelm and R. Heinrich, J. Math. Chem. **17**, 1 (1995).
[11] Th. Wilhelm and R. Heinrich, J. Math. Chem. **19**, 111 (1996).
[12] T. Ohta, Y. Hayase, and R. Kobayahi, Phys. Rev. E **54**, 6074 (1996).
[13] P. Strasser, O. E. Rössler, and G. Baier, J. Chem. Phys. **104**, 9974 (1996).
[14] G. Baier and S. Sahle, J. Theor. Biol. **193**, 233 (1998).
[15] J. Ackermann, B. Wlotzka, and J. S. McCaskill, Bull. Math. Biol. **60**, 329 (1998).
[16] T. Kirner, J. Ackermann, R. Ehricht, and J. S. McCaskill, Biophys. Chem. **79**, 163 (1999).
[17] D. Y. Kwoh, G. R. Davis, K. M. Whitefield, H. L. Chappelle, L. J. DiMichele, and T. R. Gingeras, Proc. Natl. Acad. Sci. USA **86**, 1173 (1989).
[18] J. C. Guatelli, K. M. Whitefield, K. J. Barringer, D. Y. Kwoh, D. D. Richman, and T. R. Gingeras, Proc. Natl. Acad. Sci. **87**, 1874 (1990).
[19] E. Fahy, D. Y. Kwoh, and T. R. Gingeras, PCR Methods Appl. **1**, 25 (1991).
[20] J. Compton, Nature **350**, 91 (1991).
[21] J. W. Romano, R. N. Shurtliff, M. G. Sarngadharan, and R. Pal, J. Virol. Meth. **54**, 109 (1995).
[22] G. T. Walker, M. C. Little, J. G. Nadeau, and D. D. Shank, Proc. Natl. Acad. Sci. USA **89**, 392 (1992).
[23] N. Paul and G. F. Joyce, Proc. Natl. Acad. Sci. USA **99**, 12733 (2002).
[24] M. Levy and A. D. Ellington, PNAS **100**, 6416 (2003).
[25] R. Ehricht, T. Ellinger, and J. S. McCaskill, Eur. J. Biochem. **243**, 358 (1997).
[26] R. Ehricht, T. Kirner, T. Ellinger, P. Foerster, and J. S. McCaskill, Nucleic Acids Res. **25**, 4697 (1997).
[27] B. Wlotzka and J. S. McCaskill, Biol. Chem. **4**, 25 (1997).
[28] T. Ellinger, R. Ehricht, and J. S. McCaskill, Chem. Biol. **5**, 729 (1998).
[29] R. Bräutigam, D. Steen, R. Ehricht, and J. S. McCaskill, Isothermal biochemical amplification in miniaturized reactors with integrated micor valves. In: Microreaction Technology, Springer, Berlin 1999; Proceedings of the third International Conference on Microreaction Technology, Frankfurt a. M., April 18 – 21, 1999.
[30] Th. Kirner, J. Ackermann, D. Steen, R. Ehricht, Th. Ellinger, P. Foerster, and J. S. McCaskill, Chem. Eng. Sci. **55**, 245 (2000).
[31] Th. Kirner and J. Ackermann, J. Theor. Biol. **224**, 539 (2003).
[32] Th. Kirner, D. Steen, J. S. McCaskill, and J. Ackermann, J. Phys. Chem. B **106**, 4525 (2002).
[33] R. Hill and J. H. Merkin, IMA J. Appl. Math. **53**, 295 (1994).
[34] R. Hill and J. H. Merkin, IMA J. Appl. Math. **54**, 257 (1995).
[35] R. A. Satnoianu, J. Merkin, and S. K. Scott, Physica D **124**, 345 (1998).
[36] R. A. Satnoianu, J. Merkin, and S. K. Scott, Phys. Rev. E **57**, 3246 (1998).
[37] A. M. Turing, Phil. Trans. R. Soc. B **237**, 37 (1952).
[38] L. Yang and I. R. Epstein, Phys. Rev. Lett. **90**, 178303 (2003).
[39] H. Hildebrand, A. S. Mikhailov, and G. Ertl, Phys. Rev. Lett. **81**, 2602 (1998).
[40] T. Okuzomu and T. Ohta, Phys. Rev. E **67**, 056211 (2003).
[41] Y. Tabe and H. Yokoyama, Langmuir **11**, 4609 (1995).
[42] R. Reigada, F. Sagues, and A. S. Mikhailov, Phys. Rev. Lett. **89**, 038301 (2002).
[43] D. M. Raskin and P. A. J. de Boer, Proc. Natl. Acad. Sci. USA **96**, 4971 (1999).
[44] H. Meinhardt and P. A. J. de Boer, PNAS **24**, 14202 (2001).
[45] M. Howard, A. D. Rutenberg, and S. de Vet, Phys. Rev. Lett. **87**, 278102 (2001).
[46] K. Kruse, Biophys. J. **82**, 618 (2002).
[47] K. C. Huang, Y. Meir, and N. S. Wingreen, PNAS **100**, 12724 (2003).
[48] G. Meacci and K. Kruse, Phys. Biol. **2**, 89 (2005).

[49] M. Eigen, Naturwissenschaften **58**, 465 (1971).
[50] M. Eigen and P. Schuster, Naturwissenschaften **64**, 541 (1977).
[51] J. M. Smith, Nature **280**, 445 (1979).
[52] C. Bresch, U. Niesert, and D. Harnasch, J. Theor. Biol. **85**, 399 (1980).
[53] F. J. Dyson, J. Mol. Evol. **118**, 344 (1982).
[54] M. P. Hassell, H. N. Comins, and R. M. May, Nature **353**, 255 (1991).
[55] J. Ackermann and T. Kirner, Z. Naturforsch. **54a**, 146 (1999).
[56] M. Gebinoga and F. Oehlenschläger, Eur. J. Biochem. **235**, 256 (1996).